Classical van der Waals interactions between spherical bodies of dipolar fluid

Joakim Stenhammar*
Division of Physical Chemistry, Department of Chemistry, Lund University, P.O. Box 124, SE-221 00, Sweden

Martin Trulsson
Division of Theoretical Chemistry, Department of Chemistry, Lund University, P.O. Box 124, SE-221 00, Sweden

(Received 9 March 2011; revised manuscript received 29 April 2011; published 14 July 2011)

The van der Waals interaction free energy A_{int} between two spherical bodies of Stockmayer fluid across a vacuum is calculated using molecular simulations and classical perturbation theory. The results are decomposed into their electrostatic and Lennard-Jones parts, and the former is shown to agree excellently with predictions from dielectric continuum theory. A_{int} is decomposed into its energetic and entropic contributions and the results are compared with analytical predictions. Finally, we expand the electrostatic part of A_{int} in a multipole expansion, and show that the surprisingly good agreement between the molecular and continuum descriptions is likely due to a cancellation of errors coming from the neglect of the discrete nature of the fluid within the dielectric description.

DOI: 10.1103/PhysRevE.84.011117 PACS number(s): 05.20.Jj, 77.22.Ej, 87.15.hg

I. INTRODUCTION

The understanding of van der Waals (vdW) forces between macroscopic bodies is a long-standing issue in colloidal science, due both to the fundamental interest and the many applications of these interactions [1–3]. The traditional treatments of vdW interactions, most notably that due to Lifshitz and coworkers [4], treat the quantum-mechanical (dispersion) and classical (permanent dipole) contributions to the total interaction free energy on equal grounds. Within Lifshitz' approach, the total interaction is calculated from the frequency-dependent relative permittivity $\varepsilon(i\xi)$ of the interacting materials, thus taking into account both classical and quantum-mechanical contributions to the interaction free energy. It is, however, possible to obtain expressions for the interaction between purely classical bodies by taking the appropriate limits of the Lifshitz expression, leading to an interaction free energy that depends solely on the static relative permittivity $\varepsilon(0)$ [5–8].

The interaction between bodies composed of permanent dipoles, which corresponds to the classical limit of Lifshitz theory, has not, however, been extensively studied in the past. In the 1980s, the force between planar dielectric surfaces with adsorbed dipoles was calculated using perturbation theory, integral equation theory, and Monte Carlo (MC) simulations [9–12]. In a recent study [8], expressions for the interaction between spherical bodies of classical dipoles, described through their static relative permittivity $\varepsilon(0)$, were derived within the framework of dielectric continuum theory. In the present contribution, we will calculate the interaction free energy across a vacuum between two spherical bodies of a simple dipolar model fluid using a combined MC and perturbation theory approach. The results will be compared with analytical predictions as well as decomposed into its energetic and entropic contributions. The analysis is restricted to the classical (zero-frequency) regime of the vdW interaction. However, dispersion forces are included in a semi-empirical way through generic Lennard-Jones interactions.

*joakim.stenhammar@fkem1.lu.se

II. CLASSICAL PERTURBATION THEORY

As a basis for our analysis, we will consider two subsystems labeled 1 and 2, each containing N particles. The configuration integral Z_{12} for the combined system is given by

$$Z_{12} = \int \cdots \int \exp\left[-\beta V\left(\{\mathbf{x}_i^{(1)}\},\{\mathbf{x}_j^{(2)}\}\right)\right] d\{\mathbf{x}_i^{(1)}\} d\{\mathbf{x}_j^{(2)}\}, \tag{1}$$

where $\beta = (kT)^{-1}$ is the inverse thermal energy and $\mathbf{x}_i^{(n)}$ represents all degrees of freedom of the ith particle ($i,j \in \{1,\ldots,N\}$) in subsystem n. Following the classical exposition by Zwanzig [13], we now decompose the total interaction potential $V(\{\mathbf{x}_i^{(1)}\},\{\mathbf{x}_j^{(2)}\})$ into three parts describing the internal couplings V_{11} and V_{22} within the two subsystems and the interaction V_{12} between them, i.e.,

$$V = V_{11}\left(\{\mathbf{x}_i^{(1)}\}\right) + V_{22}\left(\{\mathbf{x}_j^{(2)}\}\right) + V_{12}\left(\{\mathbf{x}_i^{(1)}\},\{\mathbf{x}_j^{(2)}\}\right). \tag{2}$$

At infinite separation between the subsystems, $V_{12} = 0$ and the configuration integral simply reduces to the product of the configuration integrals of the uncoupled subsystems, i.e., $Z_{12} = Z_1 Z_2$. The use of this fact, together with Eqs. (1) and (2) and some fundamental statistical-mechanical concepts, enables us to express the free energy of interaction A_{int} between the two subsystems as [13,14]

$$\beta A_{\text{int}} = -\ln \frac{Z_{12}}{Z_1 Z_2} = -\ln\langle \exp\left[-\beta V_{12}\right]\rangle_0, \tag{3}$$

where the subscript 0 denotes an average evaluated over the uncoupled subsystem configurations. Equation (3) is strictly exact, although useful in practice only when the overlap between the configuration spaces of the coupled and uncoupled systems is not too small. For sufficiently small values of $|\beta\langle V_{12}\rangle|$, we may also express Eq. (3) as a power series in β, according to

$$\begin{aligned}\beta A_{\text{int}} &= -\sum_{n=0}^{\infty} \frac{\omega_n}{n!}(-\beta)^n \\ &\approx \beta\langle V_{12}\rangle_0 - \frac{\beta^2}{2}\left[\left\langle V_{12}^2\right\rangle_0 - \langle V_{12}\rangle_0^2\right],\end{aligned} \tag{4}$$

where we have put in explicit expressions for the two first expansion coefficients ω_n. It should be noted that for interactions involving dipolar particles, $\langle V_{12}\rangle_0 = 0$ by symmetry, and thus the right-hand side of Eq. (4) represents the leading-order contribution to A_{int}.

For a pairwise additive intermolecular potential v, V_{12} is simply given by

$$V_{12}\left(\{\mathbf{x}_i^{(1)}\},\{\mathbf{x}_j^{(2)}\}\right) = \sum_{i,j=1}^{N} v\left(\mathbf{x}_i^{(1)},\mathbf{x}_j^{(2)}\right), \tag{5}$$

and can easily be evaluated from, for example, computer simulations. Alternatively, one may use the approach taken in Ref. [8] and express the electrostatic part $V_{12}^{(\text{el})}$ of V_{12} as a double multipole expansion of the electrostatic potentials of the two subsystems. Thus, Eq. (5) is replaced by

$$V_{12}\left(\{\mathbf{x}_i^{(1)}\},\{\mathbf{x}_j^{(2)}\}\right) = \sum_{\ell_1=0}^{\infty}\sum_{\ell_2=0}^{\infty} V\left(\mathbf{Q}_{\ell_1}^{(1)},\mathbf{Q}_{\ell_2}^{(2)}\right), \tag{6}$$

where $\mathbf{Q}_\ell^{(n)}$ denotes the 2^ℓ-pole tensor of subsystem n, and the $\ell = 0$ terms vanish for subsystems of zero net charge. One obvious advantage of using the expansion of Eq. (6) rather than Eq. (5) for calculating V_{12} from a computer simulation is that the former approach only uses a single loop over the N particles to calculate each $\mathbf{Q}_\ell$, whereas the latter requires a double loop, leading to an $\mathcal{O}(N^2)$ rather than an $\mathcal{O}(N)$ scaling behavior. This reasoning, however, only holds for separations between the subsystems where Eq. (6) converges reasonably fast.

III. MODEL AND METHODS

In the present study, we take as our subsystems two equally sized spherical bodies, each composed of $N = 10\,000$ particles. The particles are confined by a hard cavity wall of radius $R_{\text{conf}} = 40.018$ Å acting on the particle centers. The intermolecular potential is a so-called Stockmayer potential, composed of a Lennard-Jones (LJ) and a dipolar part, according to

$$v(\mathbf{x}_i,\mathbf{x}_j) = v_{\text{LJ}} + v_{\text{dip}}, \tag{7}$$

with

$$v_{\text{LJ}}(r_{ij}) = 4\epsilon_{\text{LJ}}\left[\left(\frac{\sigma_{\text{LJ}}}{r_{ij}}\right)^{12} - \left(\frac{\sigma_{\text{LJ}}}{r_{ij}}\right)^{6}\right], \tag{8}$$

and

$$v_{\text{dip}}(\mathbf{x}_i,\mathbf{x}_j) = \frac{1}{4\pi\varepsilon_0}\left[\frac{\boldsymbol{\mu}_i\cdot\boldsymbol{\mu}_j}{r_{ij}^3} - \frac{3(\boldsymbol{\mu}_i\cdot\mathbf{r}_{ij})(\boldsymbol{\mu}_j\cdot\mathbf{r}_{ij})}{r_{ij}^5}\right]. \tag{9}$$

In the above equations, $\boldsymbol{\mu}_i$ represents the dipole of particle i, $\mathbf{r}_{ij}$ is the vector pointing from particle i to particle j, $r_{ij} = |\mathbf{r}_{ij}|$, and ϵ_{LJ} and σ_{LJ} are the LJ parameters [15].

The thermodynamic properties of the unperturbed subsystems were determined by performing an MC simulation of *one* subsystem, saving a subset of the particle positions and orientations to disk. From this set, subsystem configuration pairs were chosen at random and mutually translated to a given separation. The electrostatic part $A_{\text{int}}^{(\text{el})}$ of the interaction free energy was then sampled as a function of the separation between the subsystems using (i) the exact expression of Eq. (3) with V_{12} given by Eqs. (5) and (9), (ii) the leading-order perturbation expression of Eq. (4) using the same expression for V_{12}, and (iii) Eq. (3) together with the multipole expansion of Eq. (6) to describe V_{12} using three different truncations ℓ_{max}. In addition to this, the LJ part $A_{\text{int}}^{(\text{LJ})}$ of the interaction free energy was sampled using Eq. (3) together with the pair potential from Eq. (8). The direct interaction energy U_{int} was also sampled for both the LJ and the electrostatic parts of the pair potential using standard Boltzmann-weighted averages, i.e.,

$$\beta U_{\text{int}} = \frac{\sum_s \beta V_{12}^{(s)} \exp\left[-\beta V_{12}^{(s)}\right]}{\sum_s \exp\left[-\beta V_{12}^{(s)}\right]}, \tag{10}$$

where $V_{12}^{(s)}$ represents the value of V_{12} in configuration s and the sums run over all sampled configurations. For all separations considered, $A_{\text{int}}^{(\text{el})}$ and $A_{\text{int}}^{(\text{LJ})}$ were checked to be essentially (within ~5%) uncorrelated with each other, meaning that the total interaction free energy merely equals the sum of the two contributions. Further information about the model system and calculations is given in the Appendix.

In order to map the results obtained using our molecular model onto the dielectric continuum model of Ref. [8], reasonable values of the dielectric radius a and static relative permittivity ε have to be defined within the framework of the molecular model. However, since the properties calculated from the dielectric model are largely independent of ε for high-dielectric media, we chose to use the approximative value $\varepsilon = 80$ throughout, leaving the dielectric radius a as the only fitting parameter. In accordance with what has been observed before [16], $a = R_{\text{conf}} + \delta$, where δ is on the order of half a molecular radius, due to the possibility of the particles to slightly protrude beyond the confining surface, since this acts on the particle centers. A schematic picture of the molecular model system is given in Fig. 1.

IV. RESULTS AND DISCUSSION

In Fig. 2(a), the electrostatic part $A_{\text{int}}^{(\text{el})}$ of the interaction free energy is shown, obtained using the exact and perturbation approaches described above. The optimum value of the fitting parameter was found to be $\delta = 0.73$ Å. From this figure, we observe that (i) the results obtained using the exact expression Eq. (3) show an excellent agreement with the dielectric continuum results, although there is a small discrepancy at the shortest separations considered, and (ii) the leading-order perturbation results Eq. (4) exhibit a good agreement with the exact ones for $D/a \geqslant 0.1$, below which the perturbation results start to underestimate $A_{\text{int}}^{(\text{el})}$. The first observation indicates that the molecular model system is accurately described by a dielectric continuum approximation down to very small separations; the smallest separations considered here correspond to a minimum particle-particle separation of about 2.2 Å, which is less than one LJ diameter. Observation (ii) is in agreement with the fact that the perturbation expansion of Eq. (4) is no longer accurate for large values of $|\beta A_{\text{int}}|$.

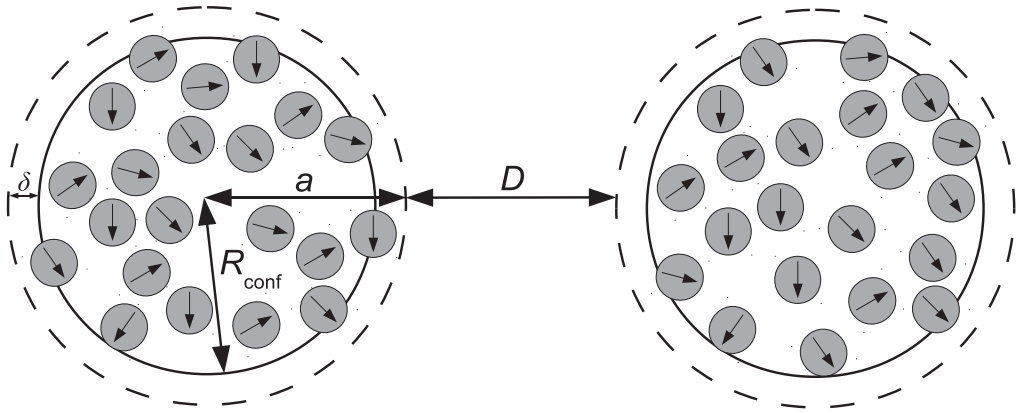

FIG. 1. Schematic picture of the molecular system, together with definitions of relevant parameters.

Figure 2(b) shows results obtained using the multipole expansion of Eq. (6) with truncations of $\ell_{\max} = 1,2$, and 3, using the value of δ (0.73 Å) obtained from the fitting in Fig. 2(a). Clearly, when including contributions up to the octupole-octupole interaction, the multipole expansion Eq. (6) grossly underestimates $A_{\text{int}}^{(\text{el})}$ for all but the largest separations considered. In other words, the description of a body composed of molecular dipoles through its fluctuating multipole moments yields a slowly converging sum, and $A_{\text{int}}^{(\text{el})}$ is underestimated by more than an order of magnitude at small separations when including multipole moments with $\ell \leqslant 3$. Furthermore, the agreement between the molecular and continuum models is still satisfactory, but there is a slight overestimation of $A_{\text{int}}^{(\text{el})}$ in the dielectric model for $\ell_{\max} = 2$ and 3. As a further indication of the slow convergence speed of Eq. (6), within the dielectric continuum formalism, truncation values of $\ell_{\max} = 500$ and 50 were needed to reach converged values (within $\sim 6 \times 10^{-4} kT$) of $A_{\text{int}}^{(\text{el})}$ for $D/a = 0.01$ and 0.1, respectively. [8] An interesting analogy can be drawn to the dispersion interaction between two quantum-mechanical polarizable bodies, such as two noble gas atoms. In this case, the interaction is often approximated using only dipole polarizabilities, and including multipole polarizabilities with $\ell \leqslant 4$ usually gives a quantitatively accurate description of the interaction [17]. Thus, there is a tremendously quicker convergence of the multipole expansion in the quantum-mechanical case, due to the large excitation energies involved in creating higher-moment fluctuations. In the case of classical polarizabilites, however, all fluctuations are, by definition, assumed to be thermally excited, and thus high-ℓ fluctuations also contribute significantly to the interaction (free) energy.

The total value and the attractive part (i.e. only the r^{-6} term) of $A_{\text{int}}^{(\text{LJ})}$ are presented in Fig. 3. Since the LJ potential is a way of representing the dispersion and short-range repulsion interactions in a semi-empirical manner, it is not feasible to try to map the LJ results onto any analytical theory (e.g. Lifshitz theory) obtained from fundamental principles. However, we note that the total LJ interaction is about an

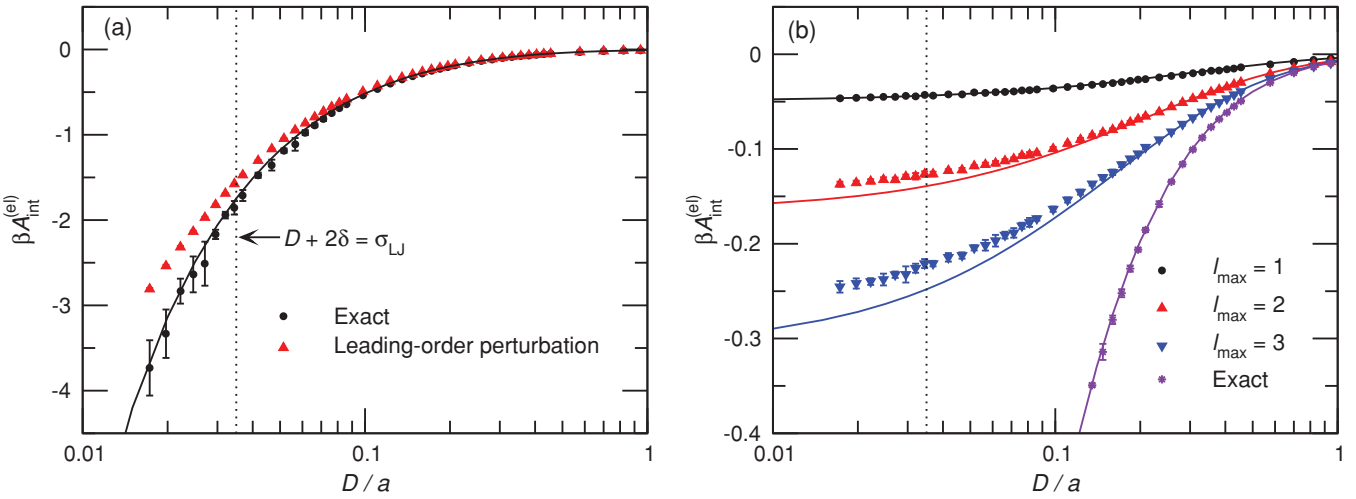

FIG. 2. (Color online) The electrostatic part $A_{\text{int}}^{(\text{el})}$ of the interaction free energy, calculated using (a) Eq. (3) (black symbols) and Eq. (4) (red symbols), and (b) Eq. (6) using three values of the truncation $\ell_{\max}$. The solid curves represent dielectric continuum results [8], and the dotted vertical lines indicate where $D + 2\delta = \sigma_{\text{LJ}}$, corresponding to the separation where particles in different bodies may start to overlap. In all cases, $\delta = 0.73$ Å and $\varepsilon = 80$ were used for the fittings to the dielectric continuum results. The error bars represent one standard deviation.

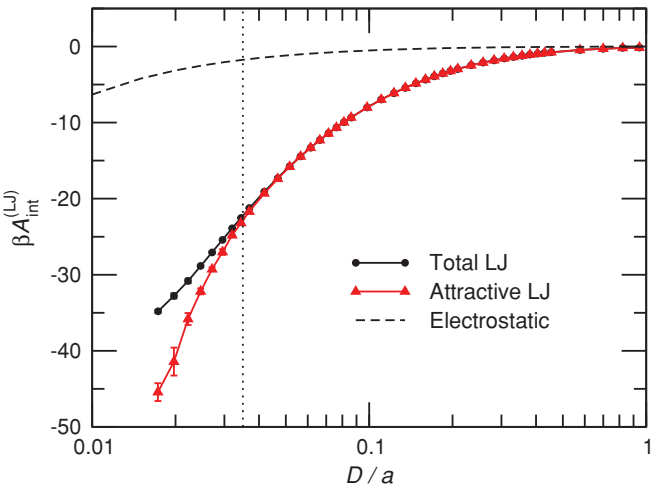

FIG. 3. (Color online) The total (black) and attractive (red) parts of $A_{\text{int}}^{(\text{LJ})}$, calculated using Eq. (3). The dashed line represents the dielectric continuum results for the electrostatic interaction [black solid line in Fig. 2(a)], and the dotted black line as in Fig. 2. The error bars represent one standard deviation.

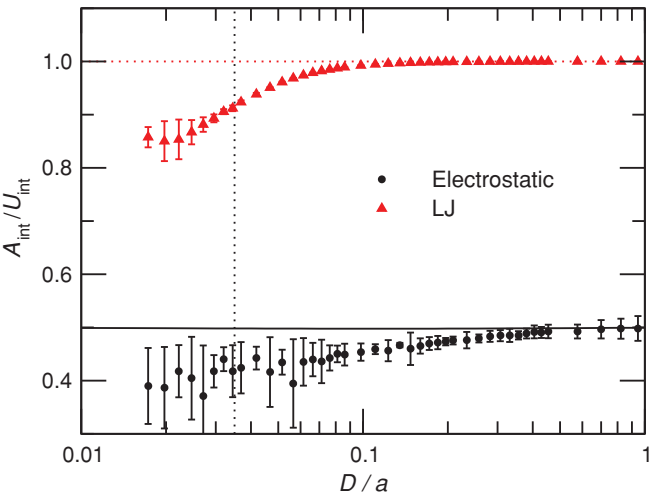

FIG. 4. (Color online) The ratio $A_{\text{int}}/U_{\text{int}}$ for the electrostatic (black symbols) and LJ (red symbols) parts of the interaction. The solid black line gives analytical dielectric continuum results [8], the dotted red line shows $A_{\text{int}}/U_{\text{int}} = 1$, and the dotted black line as in Fig. 2. The error bars represent one standard deviation.

order of magnitude stronger than the electrostatic part of the interaction free energy, which should be compared with the "internal" couplings (corresponding to $\langle V_{11}\rangle_0$ and $\langle V_{22}\rangle_0$ in the present notation) where the magnitude of the electrostatic energy is about 20% *larger* than the LJ energy (-4.25×10^4 and $-3.58 \times 10^4 kT$, respectively). The strong dominance of the LJ interactions is, however, in qualitative agreement with the fact that dispersion interactions usually dominate the vdW interaction between bodies across vacuum or air [3]. With that said, it should also be mentioned that the LJ model cannot be expected to accurately account for dispersion interactions between real bodies, since these are indeed not pairwise additive. We also note that the attractive r^{-6} part and the total LJ interaction are identical down to separations of $D/a \sim 0.05$, where the short-range r^{-12} repulsion starts to set in.

In order to study the energetic and entropic contributions to A_{int}, the ratio $A_{\text{int}}/U_{\text{int}}$ was calculated for the electrostatic and LJ contributions to the interaction. The results are shown in Fig. 4. Examining the results for the electrostatic interaction, there seems to be a systematic overestimation of $A_{\text{int}}/U_{\text{int}}$ in the dielectric continuum model as compared to the molecular description, which is a discrepancy that seems to increase as the separation decreases. Thus, the relative entropic penalty of correlating the polarization fluctuations of the two bodies is higher in the molecular system than what is predicted by dielectric theory. This can be explained by the molecular graininess and discreteness present in the molecular description, which requires a stronger correlation between the bodies to find the optimal configurations, thus leading to a larger entropic penalty than in the continuum description. It should also be noted that the dielectric continuum result is close (within ~0.5%) to the classical linear response result $A_{\text{int}}/U_{\text{int}} = 1/2$ [8]. For the LJ contribution, $A_{\text{int}}/U_{\text{int}} \approx 1$ at large separations, which is a consequence of the fact that the LJ potential, unlike the electrostatic interaction, is isotropic on length scales where the molecular graininess is negligible, since there is no angular dependence in the intermolecular potential. Thus, the orientations of the two bodies remain uncorrelated, and there is no entropic penalty involved in the interaction. At shorter separations, however, the nonuniform density of the two bodies becomes apparent, and they start to somewhat correlate their orientations in order to find the optimal configurations, just as in the case of the electrostatic interaction. The reason that the effects of discreteness seem to set in earlier (i.e., for larger separations) for the electrostatic interaction than for the LJ interaction is that the former, on the molecular level, decays as r^{-3} for short and r^{-6} for long separations, whereas the LJ potential decays as r^{-6} at all separations.

V. CONCLUSIONS

In the present contribution, we have presented results from an investigation of the vdW interaction between two spherical bodies of Stockmayer fluid using Monte Carlo simulations and statistical-mechanical perturbation theory. The main finding is that the electrostatic part of the free energy of interaction between the two bodies shows excellent agreement with dielectric continuum results. Furthermore, the Lennard-Jones part of A_{int} was shown to be about one order of magnitude larger than the electrostatic interaction. Finally, we noted that dielectric continuum theory slightly underestimates the entropic penalty associated with correlating the electrostatic fluctuations of the two bodies, as compared to the molecular system.

Although the agreement between simulation data and dielectric continuum theory is in general good, and in many cases excellent, it is interesting to analyze the nature of the discrepancies that do exist. One puzzling fact is the excellent agreement between theory and simulation when calculating the exact values of $A_{\text{int}}^{(\text{el})}$ [Fig. 2(a)], an agreement that holds down to separations of molecular dimensions. On the other hand, the dielectric continuum model seems to overestimate $A_{\text{int}}^{(\text{el})}$

obtained from the multipole expansion approach [Fig. 2(b)], an overestimation that increases with increasing values of the truncation $\ell_{\max}$, at least for $\ell_{\max} \leqslant 3$. This increasing difficulty of the molecular system to fully (compared to the dielectric case) develop electrostatic fluctuations of increasing order ℓ is in accordance with what has been observed before for subvolumes inside a bulk fluid, in those cases for $\ell \leqslant 4$ [16,18]. However, the lack of interaction energy for low values of ℓ clearly has to be compensated by "super-dielectric" contributions from higher terms in the multipole expansion in order to be consistent with the good agreement between theory and simulation for the exact calculation of $A_{\text{int}}^{(\text{el})}$. This can be explained by the fact that for small separations, $A_{\text{int}}^{(\text{el})}$ is strongly dominated by interactions between a few particles that are very close to each other, rather than by the collective multipole moments of the whole bodies. These interactions correspond to terms of very high order in the multipole expansion, which thus compensate for the subdielectric contributions from terms of low and intermediate values of ℓ. This means that the good correspondence between the total interaction obtained from the molecular and continuum models is partly due to the cancellation of two different errors coming from the inability of dielectric continuum theory to take into account the particulate nature of the molecular fluid. This is also the reason behind the underestimation of the entropic penalty for correlating the fluctuations of the two bodies present in the dielectric continuum theory.

It should be mentioned that the confining hard-wall potential used here was chosen due to its technical convenience rather than on physical grounds. Indeed, for the smallest separations considered, we would expect considerable deviations from spherical geometry, which can strongly affect the magnitude of the vdW interactions [19]. One obvious improvement, if one wants to describe a "real" droplet, would be to instead simulate a spontaneously condensed droplet of dipolar particles, which would then be in equilibrium with its own vapor. This approach would clearly lead to the possibility of larger shape fluctuations, however, leading to further difficulties in defining the sizes of and separation between the bodies. Furthermore, this would lead to problems when trying to map the results onto dielectric continuum results, which was one of the main objects of this study, since the continuum results were obtained using an idealized spherical geometry. With that said, we still believe that the present choice of confining boundary conditions gives a qualitatively correct picture of the fluctuation interaction between two real fluid bodies.

ACKNOWLEDGMENTS

Enlightening discussions with Gunnar Karlström and Per Linse are gratefully acknowledged. This work was partly (J.S.) financed by the Swedish Research Council (VR) through the Linnaeus grant for the Organizing Molecular Matter (OMM) Center of Excellence.

APPENDIX: MODEL AND CALCULATION DETAILS

For the model system, the LJ parameters $\sigma_{\text{LJ}} = 2.8863$ Å and $\epsilon_{\text{LJ}} = 1.970\,23$ kJ mol^{-1} were used, together with the dipole moment $\mu = 0.343\,97e$ Å (corresponding to 0.65 atomic units). The temperature was kept constant at $T = 315.8$ K. In reduced units, the system was characterized by the quantities $\mu^* \equiv \mu/(4\pi\varepsilon_0\epsilon_{\text{LJ}}\sigma_{\text{LJ}}^3)^{1/2} = 1.863$ and $T^* \equiv kT/\varepsilon_{\text{LJ}} = 1.333$. The specifications of the model system are identical to those employed in Ref. [16].

The MC simulations were carried out in the canonical (constant N,V,T) ensemble employing the molecular simulation package MOLSIM [20] with translational and rotational displacement parameters of 0.7 Å and 25 degrees, respectively. The simulation extended over 2×10^6 MC steps, each involving one trial move per particle. Particle positions and orientations were saved every 1000 MC steps, yielding 2×10^3 saved configurations in total. All interparticle interactions were considered explicitly within the cavity, without applying any long-range correction.

Interaction energies and free energies were calculated using a Fortran 90 computer code. For each separation, 10^5 configuration pairs were chosen randomly. For each configuration pair, ten random mutual orientations of the two spheres were created, and the relevant thermodynamic parameters were sampled. The multipole tensors $\mathbf{Q}_\ell$ $(1 \leqslant \ell \leqslant 3)$ were calculated with respect to the center of each spherical subsystem using the approach described in the appendix of Ref. [18]. Statistical uncertainties were estimated by subdividing the calculations into ten equally sized blocks.

[1] D. F. Evans and H. Wennerström, *The Colloidal Domain: Where Physics, Chemistry, Biology and Technology Meet* (Wiley, New York, 1999).
[2] V. A. Parsegian, *van der Waals Forces* (Cambridge University Press, New York, 2006).
[3] J. Israelachvili, *Intermolecular & Surface Forces* (Academic, London, 1991).
[4] I. E. Dzyaloshinskii, E. M. Lifshitz, and L. P. Pitaevskii, Adv. Phys. **10**, 165 (1961).
[5] B. W. Ninham and J. Daicic, Phys. Rev. A **57**, 1870 (1998).
[6] H. Wennerström, J. Daicic, and B. W. Ninham, Phys. Rev. A **60**, 2581 (1999).
[7] H. Wennerström, Colloids Surf. A **228**, 189 (2003).
[8] J. Stenhammar, P. Linse, H. Wennerström, and G. Karlström, J. Phys. Chem. B **114**, 13372 (2010).
[9] P. Attard and D. J. Mitchell, Chem. Phys. Lett. **133**, 347 (1987).
[10] B. Jönsson, P. Attard, and D. J. Mitchell, J. Phys. Chem. **92**, 5001 (1988).
[11] P. Attard, R. Kjellander, D. J. Mitchell, and B. Jönsson, J. Chem. Phys. **89**, 1164 (1988).
[12] M. K. Granfeldt and B. Jönsson, Chem. Phys. Lett. **195**, 174 (1992).
[13] R. Zwanzig, J. Chem. Phys. **22**, 1420 (1954).
[14] D. A. McQuarrie, *Statistical Mechanics* (University Science, Mill Valley, CA, 2000).

[15] J. P. Hansen and I. R. McDonald, *Theory of Simple Liquids* (Academic, London, 2006).
[16] J. Stenhammar, P. Linse, and G. Karlström, J. Chem. Phys. **132**, 104507 (2010).
[17] N. Alves de Lima, J. Chem. Phys. **132**, 014110 (2010).
[18] J. Stenhammar, P. Linse, and G. Karlström, J. Chem. Phys. **131**, 164507 (2009).
[19] J. Klahn, W. Agterof, F. van Voorst Vader, R. Groot, and F. Groeneweg, Colloids Surf. **65**, 151 (1992).
[20] P. Linse, MOLSIM (Lund University, Sweden, 2010).